Abstract

LEVY, ANTOINE SIMON RAPHAEL. Toward the Selective Functionalization of Bimetallic Nanorods. (Under the direction of Lin He).

Over the past 30 years, the nanotechnology and nanomaterials field has undergone an exponential interest. Nano-objects are at the interface between bulk materials and atoms/molecules and share properties of both states in addition to some very attractive ones due to their unique sizes and shapes. The fields of biosensing, imaging, medical treatment, catalysis, fuel production, energy production, electronics and optics have all achieved tremendous improvement thanks to nano-objects. A lot of resources have been dedicated to understand and control the synthesis of nanoparticles yielding a vast library of particles with different sizes, shapes and compositions. More recently, multimetallic nanorods have attracted increasing interest due to the advantage to have different materials co-present on the same particle.

Selective functionalization of different sections in nanorods can lead to the combination of properties to improve their solubility, biocompatibility, spectroscopic properties, stability etc. Surprisingly little research has been done using orthogonal surface chemistry for pre-designed self-assembly of nanorods in spite of its dramatic impacts in a context where it becomes harder and harder to mechanically assemble small electronic compound.

In this research project, I have developed an approach to selectively derivatize the gold surface using thiolated molecules and the nickel portion using phosphonic acid. The prepared functioning scheme can later be used for oligonucleotide attachment and subsequently controlled assembly of bimetallic nanorods on DNA origami films. The process is developed on metal-coated macroscopic thin films to ease the challenge coating characterization. Both X ray photoelectron spectroscopy and ellipsometry are used for qualitative and quantitative measurements of resulting coatings. Multimetallic nanorods are synthesized with various size-controlled blocks of nickel and gold using an alumina template and chronopotentiometry. They are characterized by energy dispersive

spectroscopy and scanning electron microscopy imaging. Selective coupling of thiolated DNA to the particle surface is also attempted.

Toward the Selective Functionalization of Bimetallic Nanorods

by
Antoine Levy

A thesis submitted to the Graduate Faculty of
North Carolina State University
in partial fulfillment of the
requirements for the degree of
Master of Science

Chemistry

Raleigh, North Carolina

2015

APPROVED BY:

Dr. Edmond Bowden	Dr. Christopher Ashwell
Dr. Lin He Committee Chair	Dr. Felix Castellano

Dedication

To my friends and family who supported me all the way to where I stand today. To my grandfather who never stopped reminding me that I can do better. To my father whose stubbornness helped me developed my interest in science. I wish you could have seen this day.

“Emotion, yet peace.

Ignorance, yet knowledge.

Passion, yet serenity.

Chaos, yet harmony.”

Biography

Born: September the 18th, 1988 in Agen (France)

Parents: Marie Thérèse Rouire and André Levy

Siblings : Louisa Levy, Sigoline Levy and Jean-Baptiste Levy

Highschool : Jean-Baptiste De Baudre (2007)

Technician diploma : IUT Paul Sabatier (2009)

Diploma of engineer : CPE Lyon (2015)

Acknowledgements

I would like to thank my advisor Lin He for her guidance over the past years. Although very busy and often off site, she has always been available to help me in the direction of my research. A good advisor is important but cheerful coworkers are equally important and for their help and shared laughs, I thank Tara Moening, Tom Chase, Victoria Brown, Kangshu Zhan and Nathalia Ortiz.

I would like to thank the members of the Gorman group and the Franzen group for their help and explanations with instrumentation and chemical finding.

For his help with electrochemistry, I thank Dr Edmond Bowden and for the guidance about SAM and ellipsometry, I thank Dr Gorman. Fred Stevie also has my thanks for his prompt help with XPS analysis.

I also thank my committee members Drs. Chris Ashwell and Felix Castellano for their overview and helpful critiques and advice.

I am very grateful to the CouchSurfing community with whom I met amazing peoples and shared incredible stories. I also thank the Krav Maga Raleigh club for all the punches, kicks, chokes, elbows that helped me relaxing after the long days spent in the lab.

Finally I would like to express my gratitude to my friends and family oversea who supported me all along my time here in the US. Their support carried me through the doubts, the fear and the sadness I encountered while being away. They did so by keeping me up to date with my homeland, making puns in French when I felt homesick and shipping survival packages in my most desperate times.

Table of Contents

List of Figures

List of Tables

List of Abbreviations

DI	dionized
DNA	deoxyribonucleic acid
DTT	dithiothreitol
EDS/EDX	Energy dispersive (X ray) spectroscopy
EDTA	ethylenediaminetetraacetic acid
NP	nanoparticle
NW	nanowire
SAM	self-assembled monolayer
SDS	sodium dodecyl sulfate
SEM	scanning electron microscopy
STEM	Scanning transmission electron microscopy
TBE	tris borate EDTA
TOF SIMS	time of flight secondary ion mass spectrometry
XPS	X-Ray Photoelectron Spectroscopy

1. Background and Significance

1.1. The increasing interest for nanorods applications

Recent developments of nano-object synthesis have led to the study of nanorods. Nanorods are a specific type of nanoparticles. They are cylindrical (length:width > 1) as opposed to most widely used spherical nanoparticles. Due to their geometric uniqueness, many exhibit different physical properties, depending of their orientations, which can be simultaneously a point of interest as well as a challenge.

Further development of nanorods led to multimetallic material in which the particles are composed of multiple distinct materials. There are many ways materials can be arranged but we will describe the two most commons. The multilayers nanorods are usually synthesize by growing a core with ligands controlling the shape and then chemically depositing layers of materials around it. The barcodes consists in a consecutive blocks of various length made from different materials. They are usually synthesized by sequential deposition of materials within a template.

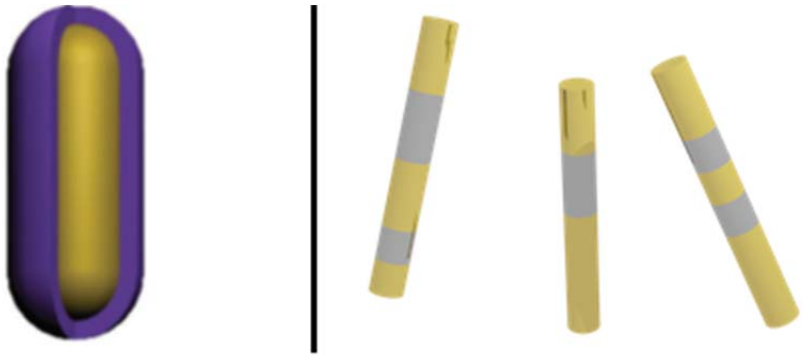

Figure 1: multilayers nanorods(left) and segmented nanobarcodes (right)[1]

Between the two, multimetallic stripped nanoparticles (i.e. nanobarcodes^{TM}, nanowires in which metals are arranged in blocks) have been the focus of many fields including (but not limited to) biosensing, catalysis and electronics.

1.1.1. Multimetallic nanoparticles for biological applications

Nanobarcodes containing noble metals (i.e. Au, Ag, Pt) have unique optical properties. The free electrons in the conducting band allow the use of near IR to exploit their plasmonic properties. By tailoring the barcodes accordingly, photons of a specific wavelength can make the electrons oscillate on the metal surface. The materials used, the size and the shape of the rods all have influences on the photons absorption frequency.[2] The surface coverage also has an influence on the plasmon which means a very simple method for biosensing can be developed just by detecting the modification in the absorbed frequencies.[3] Using the tunability offered by the control of the synthesis, various particles have been designed to absorb photons from the visible range to the near IR in which the absorbance of biological material usually weakly absorbs.[4,3] The IR absorption properties can also be exploited as cancer treatment. The nanorods can heat upon exposure to IR. By functionalizing the nanorods to make them attach to cancer cells, it is possible to locally heat the tumor and destroy it since these type of cell are highly sensitive to heated conditions.[5]

The tunability of the metallic sequence allows an easy optical detection. Our group has investigated the optical recognition of nanobarcodes in multiplexed detection of oligonucleotides using fluorescent polythiophene.[6].

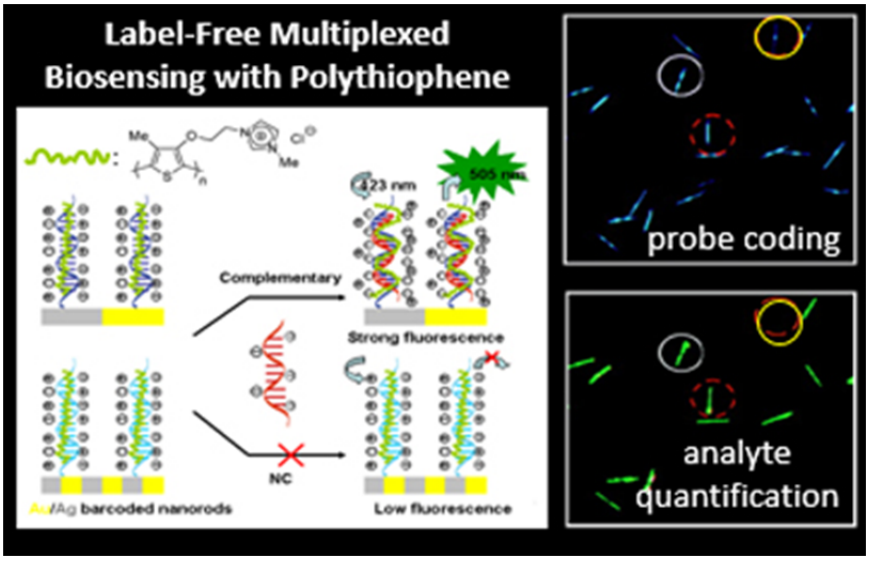

Figure 2: Use of barcodes combined with fluorescent polymer for oligonucleotides detection[7]

Briefly, silver and gold barcodes of specific motif are coated with glass. ssDNA is attached to the glass with one sequence per motif. After hybridization with analyte, polythiophenes are added. Polythiophenes are fluorescent only when the chain intercalates in the double helix structure of dsDNA. By fluorescence, it is possible to see which barcodes and sequences are present in the solution. Unlike surface based assay, nanorods can move freely in solution which increases the chance of binding events. They also have a higher surface to volume ratio so more targets can be attached. Other sensing methods have been developed for glucose detection using nanorods to enhance electrochemical detection.[8]

Gene transfection has been achieved by Leong and colleague using bimetallic nanowire. They coated on part of the nanowire with transferrin to ensure the uptake of the particles and the other part with plasmids that are released in the cell. The toxicity of nanoparticles is still under scrutiny but this is an important step for gene therapy. [9]

1.1.2. Multimetallic nanoparticles in energy production

Bimetallic nanoparticles often have better performances than the monometallic ones. This is particularly interesting for catalysis.[10] Energy harvesting and fuel production greatly benefit from the high area/volume ratio as well as multiple chemical properties from having multiple metals present on the particles.

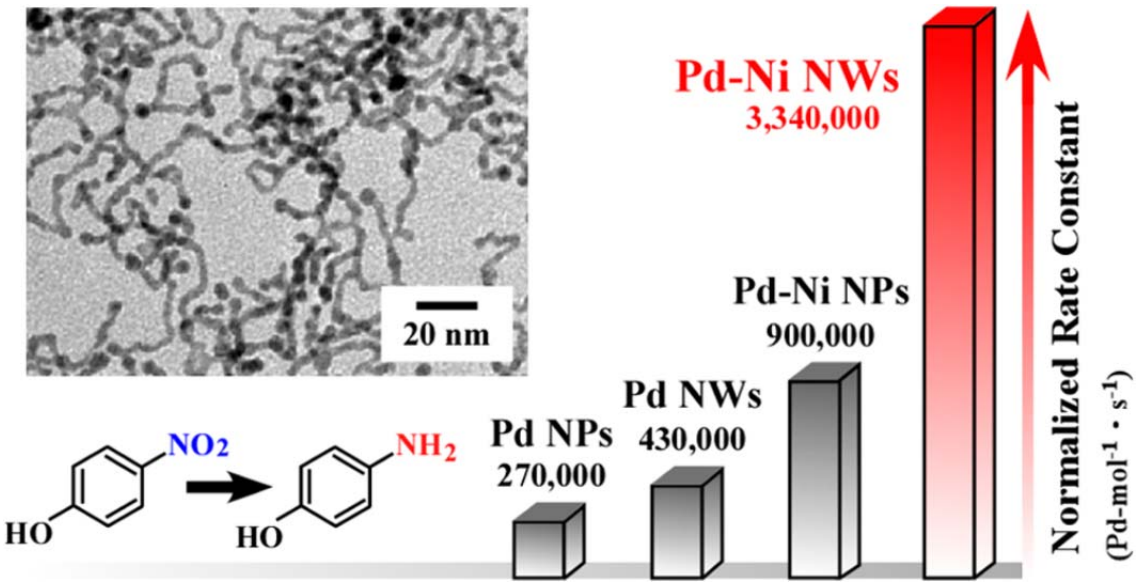

Figure 3: Pd-Ni nanowires activity vs other Pd based particles[11]

Dr. Kawai and colleagues recently developed a method to synthesize palladium-nickel nanowire and prove their increased catalytic activity in hydrogenation process compared with palladium only nanoparticles and nanowires. The method uses lower amount of palladium which would greatly decrease the cost of the catalyst.[11] On a similar idea, Yang *et al.* have developed a method to control

the growth of rhodium allow on the tip of nanorods for catalytic oxidation purpose. It is interesting to note control of the shape development of the particles in solution.[12]

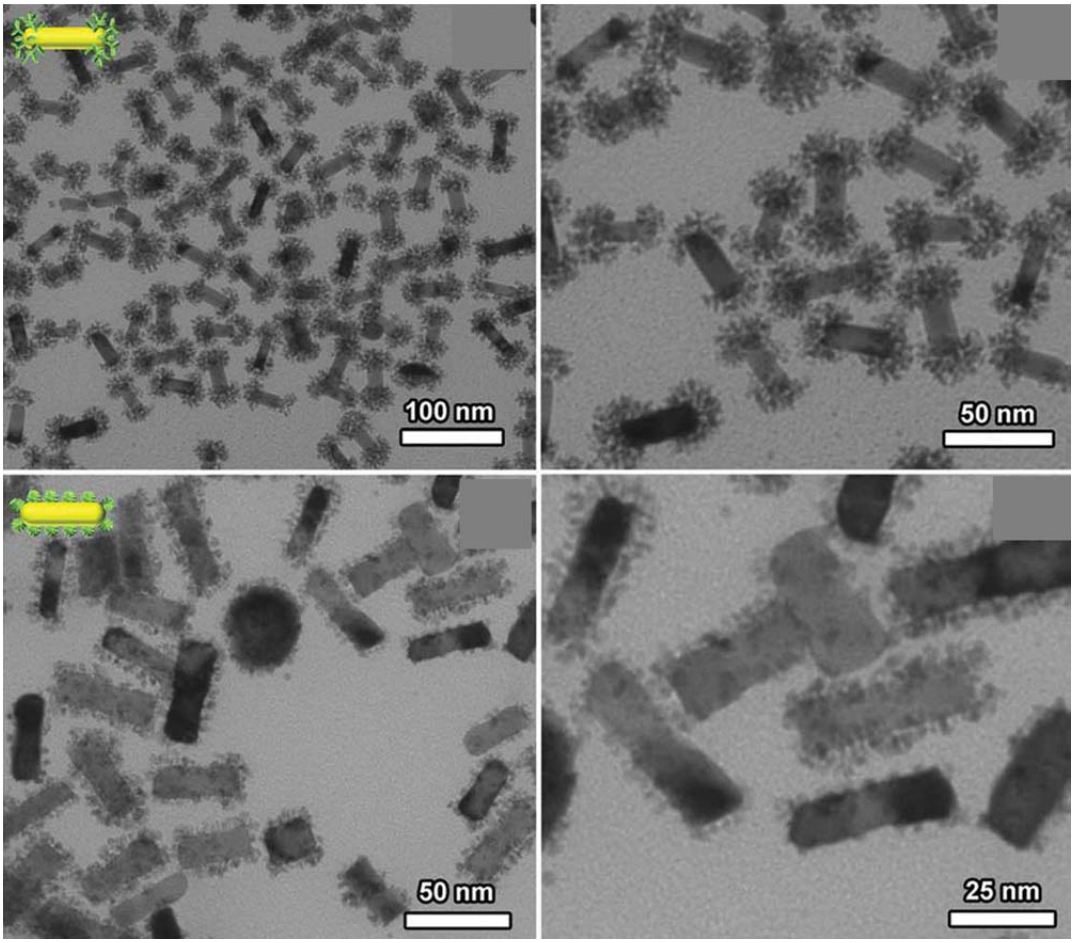

Figure 4: STEM images of different growth mods for multimetallic particles[12]

Bimetallic particles have shown promising results in fuel cell production. One of the most promising fuel cell model is based on the oxidation of methanol at low temperature (<100^{o}C). This

type of cell uses liquid and doesn't generate dangerous byproduct. The imminent depletion of fossil energy makes the development of such technology crucial. The catalysts required in this process often get poisoned by accumulation of organic impurity on the surface which makes the need of stronger oxidative power and high surface to volume ratio desirable. To this end, platinum-palladium nanoparticles have been investigated and shown promising results.[13]

It is clear that multimetallic nanostructures are getting an increasing interest from the scientific community in various field of application. In biosensing and electronic, it would be interesting to be able to control the position and orientation of such small particles and doing so mechanically is extremely challenging and costly. It is possible to use tips to move nanobject but the speed is extremely low and it would be a one by one process. Therefore, self-assembly for such materials is highly desirable.[14]

1.2. Synthesis and analysis of multimetallic particles

1.2.1. Nanorods synthesis

Nanoparticles can be synthesized in many different ways. One of the most common ways is to reduce metallic ions in solution and controlling the growth of the crystals by adjusting the conditions (temperature, concentration, ligands etc.). However, using this method, it is very hard to obtain well-ordered and size controlled multimetallic particles.[15] The most common method to obtain well defined and shaped controlled multimetallic nanorods is to deposit metals chemically or electrochemically in a template that is later removed.[16]

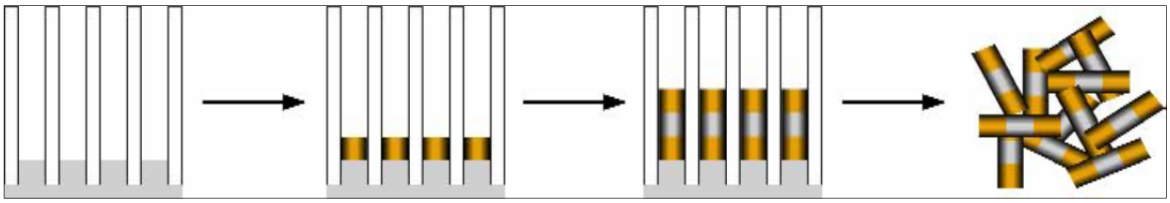

Scheme 1: Nanorods synthesis by block building using chronoamperometry[17]

The most common material for template is aluminum oxide. Porous membranes can be obtained with high homogeneity in pore size and geometry. Using these membranes allows a precise deposition that can be control on a large scale by tuning the current.[18] One side of the membrane is usually coated with a sacrificial metal layer that will ensure the contact between the electrode and the pores homogeneously. The plating solution is then applied and the size of each metallic block is controlled by the charge passed through the pores. This technique is especially useful for metal and alloys (Au, Ag, Pt, Ni, CdSe etc.).[19] Once the desired pattern is obtained, the sacrificial layer is removed and the membrane is dissolved yielding the nanorods in solution. Other methods exist to obtain other types of material. For instance, sol gel process has proved to be effective to obtain oxide blocks by hydrolyzing metal alkoxides or salt.[20]

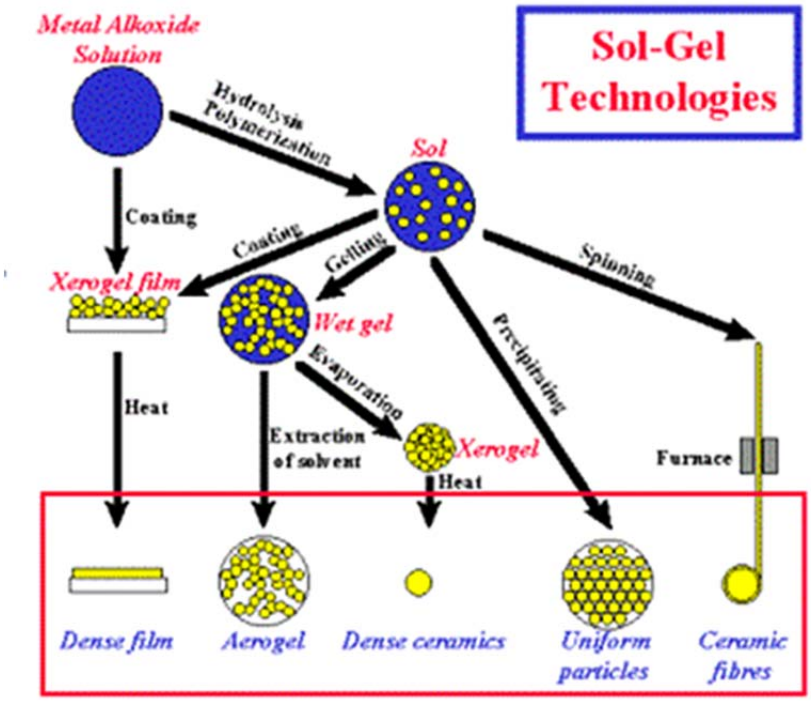

Figure 5: Sol gel process[21]

Last but not least, biological materials have been used as a template to create nanowires. Double stranded DNA can be metallized to obtain up to 12µm conductive nanowire. Kong *et al.* reported a multiplexed detection technique for tumor marker using cadmium or lead sulfide nanoparticles grown on dsDNA.[22] Other metals such as silver can be used.[23] We will emphasize how this later technique could be of interest for future application of this project.

1.2.2. Nanorods functionalization

To fully take advantage of having multicomponent particles, it is important to develop a chemistry that is selective toward specific materials. In this section, we present the main options to selectively attach organic material to the surface of the nanoparticles. Self-assembly of organic molecules on

surfaces is obtained by using various techniques and conditions. It is important to remember that surface chemistry on a particle usually offers a lesser range of applicable conditions as the particles can be destroyed by high heat or aggregate in high salt media. We will describe the organic material for SAM as follow:

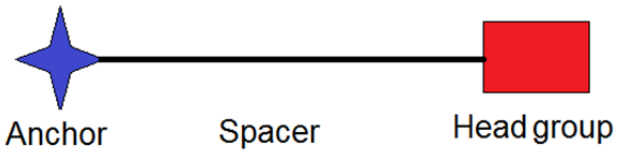

Figure 6: General description of SAM material

The anchor is the part of the molecule that is investigated to be selective toward one or another material. The spacer is, in our case, an alkyl chain of 10+ carbons (improved stability). The head group is designed to later attach oligonucleotides (carboxylic acid, biotin, and alkyne). Countless head groups have been shown to have activity toward different substrates (thiols, carboxylic acids, phosphate, alkynes, isocyanides, nitriles, organosilicons, etc).[24] We will focus on the ones showing affinity toward gold or nickel.

Perhaps one of the most well studied SAM is thiol molecule on gold. Thiol functionalization of gold has been well studied for decades.[24-25]

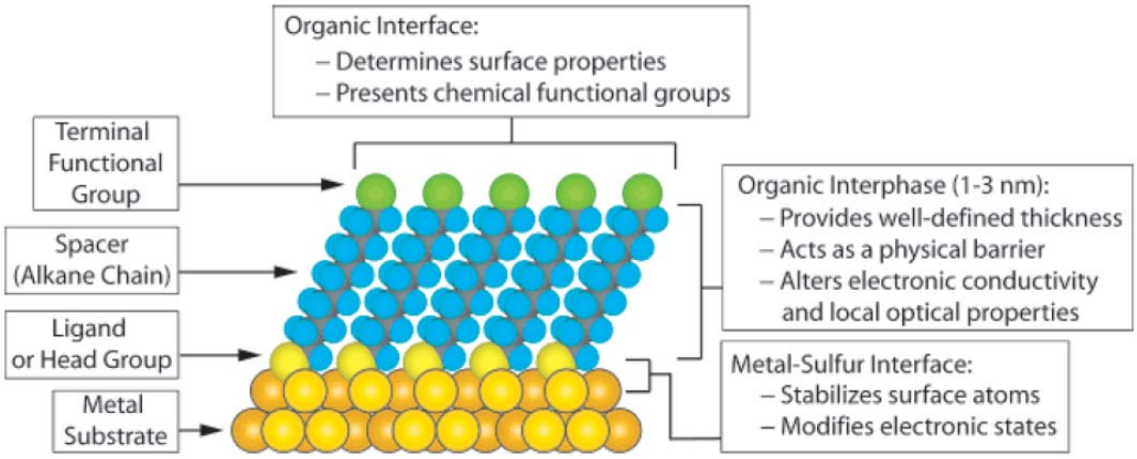

Figure 7: schematic of alkylthiolated gold surface[24]

Thiols can also functionalize other metals such as silver, copper, platinum, nickel etc. [26] Although one of the most studied, the nature of the gold-thiol bond is very complex and is still under investigation.[27] The affinity is so high though that almost all non-thiolated material will be desorbed by competitive binding.[28] However, thiols are known to have little to no reactivity t,oward nickel oxide. It is possible to attach thiol on nickel but a reducing step is necessary.[29]

There is surprisingly not a lot of literature about selective metal functionalization of gold/nickel nanorods. Native nickel, when exposed to air, forms an oxide layer.[30] Carboxylic acids are known to bind the native oxide layer of nickel.[19b, 31]

An alternative to carboxylic acids for metal oxide functionalization is the use of phosphonic acid.[32] Phosphonic acids do bind to gold as well however the thiol gold interaction is strong enough to avoid molecular exchange on the surface.[33]

1.2.3. Nanorods characterization

Three important parameters need to be distinguished when speaking about nanorods characterization: the structure, the homogeneity of the sample and the surface organization of the SAM. Since nanorods are not spherical particles, it has been observed that the UV Vis absorption profile of this type of particles depends on the aspect ratio (two different wavelength absorption peaks). Using this, it is possible to obtain information about the general aspect ratio and the dispersion of the population of the particles.[34]

Electron microscopy is usually the gold standard to obtain images of the particles. SEM is used to obtain imaging from the particles themselves. Since the electrons knocked out have different energy depending on the material they come from, it is possible to obtain a topographic image.

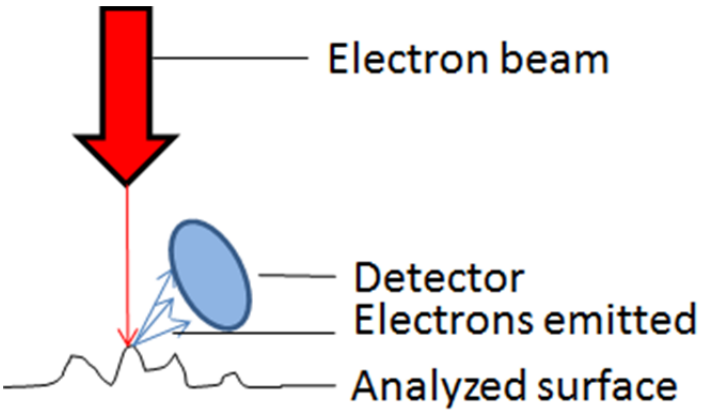

Figure 8: Diagram of SEM imaging

In addition to the topography of the surface, the electron amounts can give information about the different materials since having different energy levels would yield different electrons densities. This

helps determining the boundaries between one material and the other. SEM alone gives information about the shape of the material and eventually, the blocks composing it. It is, however unsuitable to determine the chemical composition of the blocks and it must be kept in mind that a picture of a few particles is hardly representative of the whole population.

In order to determine the composition, energy dispersive X-ray spectroscopy (EDX) is used. An electron beam knock out electrons from atoms inner electrons shells. To compensate the misbalance in charges, an electron from a higher layer loses energy by emitting an X-ray photon. The photons wavelength depends on the atoms present on the material. A chemical mapping can be obtained and overlapped with a SEM image to attribute the composition of the particles.

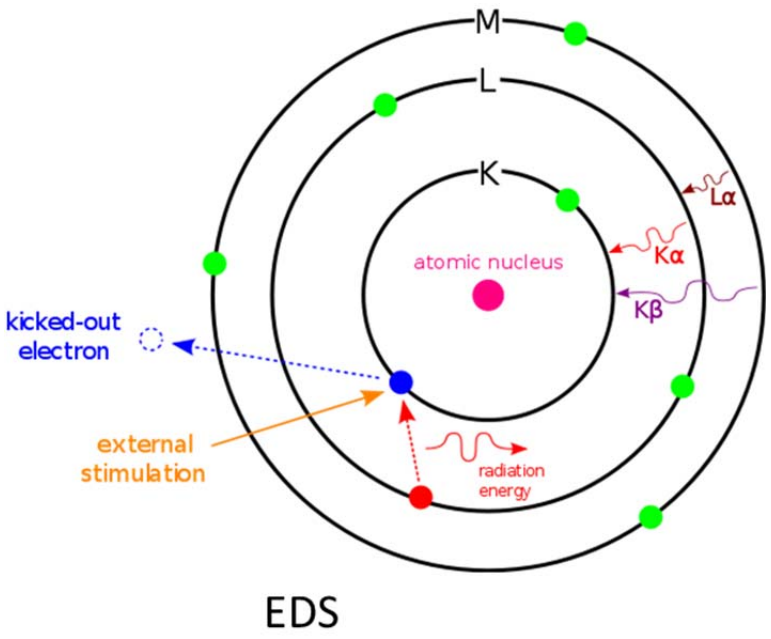

Figure 9: Illustration of X-ray emission for EDX

Now that the nanorods have been characterize, it is important to also characterize the surface of the nanorods in order to determine the location of the covering molecules. It is especially interesting when more than one material is used. Unfortunately, this requires equipment with high resolution and sensitivity since the molecules to be detected are confined and in small quantity. EDX is not sensitive enough for regular SAM molecules detection since organic molecules do not have as good of an X-ray emission yield as metals usually have. To a certain extent, it is possible to use time of flight secondary ionization mass spectrometry (TOF-SIMS) to desorb and ionize the SAM.[35]

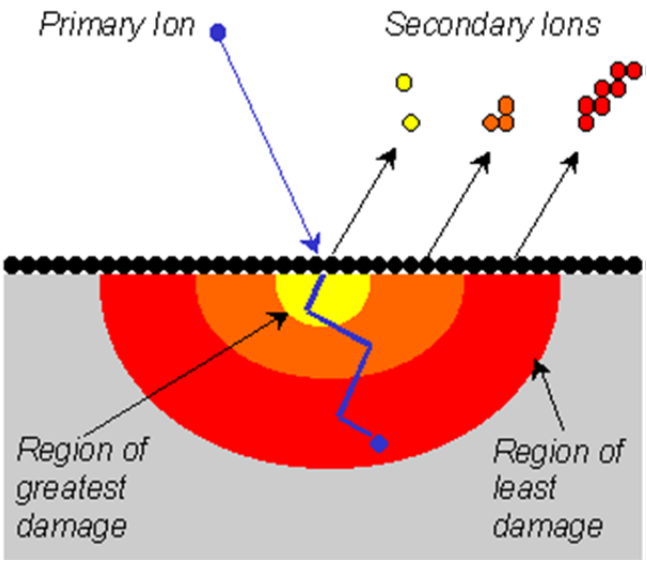

Figure 10: Diagram of the SIMS process [36]

This technique is limited in terms of resolution with current instrumentation. The resolution of current instruments is a few hundred nanometers. It is clear that direct detection is challenging.

However, indirect detection methods have been developed. The two main methods rely on attaching a tag on the surface that is easier to detect. Ding and coworker have studied the attachment of thiolated DNA to gold nanorods. They characterized the surface and prove the DNA attachment by attaching nanoparticles to the complementary strand of the sequence attached to the nanorods. This leads to a change of the topography of the nanorods which can be easily detected by SEM imaging.[37] Due to the lack of time, I was not able to use such instrumentation. Other analytical techniques will be describe in the experimental section.

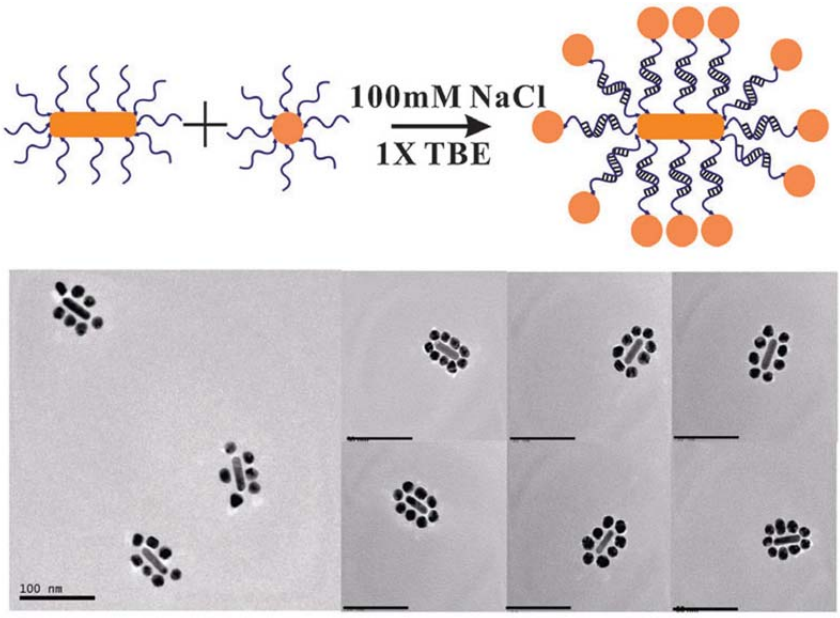

Figure 11: nanoparticles attachment to nanorods by DNA hybridization and SEM images[37]

Additional characterization approaches include indirect study of a fluorescent dye attached to the surface by selective coupling or selective adsorption.[9, 31, 38] Leong *et al* .have used this technique to observe the selective functionalization of nanowires.[9]

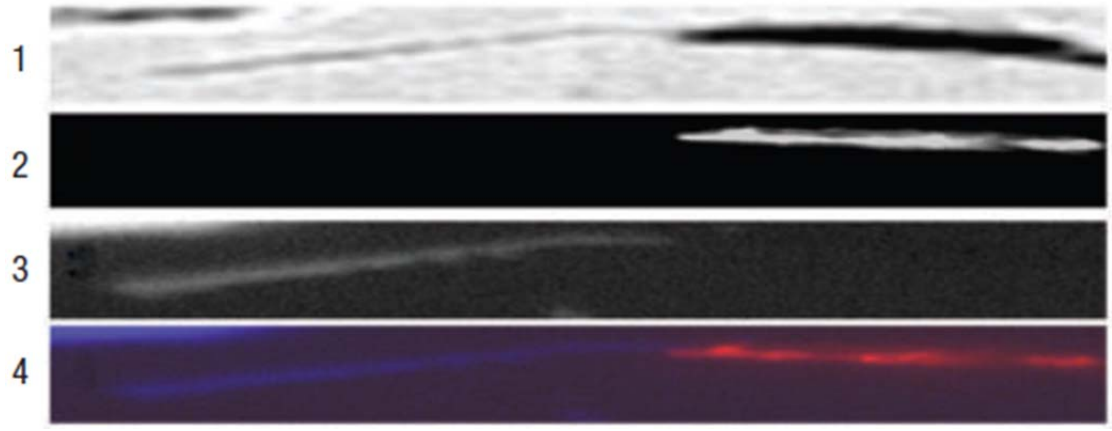

Figure 12: 1. Light microscope image of dual functionalized Au/Ni nanorod 20 µm long. 2. Fluorescence image of the rhodamine-tagged (633 nm) transferrin on the Au segment. 3. Fluorescence image of the Hoechst-stained (350/450 nm) plasmids on the Ni segment. 4. Fluorescent overlay image combining 2 and 3[9]

It should be noted that for the latest, it is possible that fluorescence quenching from the surface occur. For this reason, the nanorods used by our former group member were covered with glass (spacing between fluorophore and surface). Fluorescent quenching from metallic surface has been studied.[39] Because of the analytical challenge encountered in direct surface analysis on nanorods, it is advantageous to develop the chemistry on metal coated slides which have broader analysis technique available.

1.3. Project goal, strategy and impact

The research presented here focus on the synthesis and functionalization of bimetallic nanorods composed of gold and nickel for later self-assembly purposes. with controlled location and orientation of many different nano objects simultaneously. My research finding here can also later be used for the organization and orientation of nanorods by DNA chemically rather than mechanically.

The research project was carried out in three steps: nanorod synthesis, selective derivation of small molecules on a thin film as the model system, and DNA attachment on particles.

It is theoretically possible to functionalize a surface with DNA directly using different modified end bases; however such modified oligonucleotides are expensive and dramatically reduce the number of possibilities since genetic material is sensitive to harsh environmental conditions. To compensate this, I have developed self-assembled monolayer selectively using small molecules as the model system first.

The chemistry was also optimized on a metal thin film, which was easier to characterize. It is assumed that the chemical mechanisms are similar on a flat surface and on a rod surface. Most functionalization chemistry done on nickel surface is unsuitable to nickel particle so a solution based method needs to be developed.[40]

The last but the least I carried out kinetics studies of molecule adsorption on the metal surface and fitted the curve to the first approximation of Langmuir binding kinetics.

2. Experimental Section

2.1. Materials

Dithiothreitol, sodium dihydrogenophosphate, disodium hydrogenphosphate, potassium dihydrogenophophate, ethylenediaminetetraacetic acid, 6 mercaptohexanol, tris, 11 mercaptoundecanoic acid, 16-phosphonohexadecanoic acid, thionyl chloride, sodium dodecyl sulfate, citric acid were ordered from Sigma-Aldrich. Ethanol, triethylamine, sodium chloride, nitric acid were ordered from Fisher. Hydrogen peroxide 30% in water, ammonium hydroxide and acetonitrile were ordered from EMD chemicals. Sulfuric acid was ordered from BDH. TBE buffer 10x was ordered from Promega. The oligonucleotides were ordered from Integrated DNA technology and properties are given in table 1.

Potassium aurocyanide, silver succinate and nickel sulfamate solution were ordered from Technic. The gold slides (50 Å chromium 1000 Å gold) were ordered from EMF. Alumina oxide membranes (Anodic 0.1 μm 13 mm) were ordered from Whatman.

Table 1: DNA properties

Name	Tm (°C)	MW (g/mol)	Extinction coefficient	Sequence
DNA3	62	9439.4	282700	5' C6-S-S-C6-GGA GAC TGT TAT CCG CTC ACA ATT CCA CAC

Water was deionized using Millipore Q 50 with and APS ultra column. Dry solvent were obtain from filtration on alumina.

The potentiostat used for electrochemical deposition was a WaveNow from Pine controlled by the software Aftermath. The ellipsometry measurements were taken with an Auto EL from Rudolph research using a He-Ne laser.

2.1.1. Thin film analysis techniques

This paragraph will give a brief overview of the thin film analysis techniques used during the project. Ellipsometry is a surface analysis that is based on polarized light travel time to obtain information about the thickness of adsorbs material.

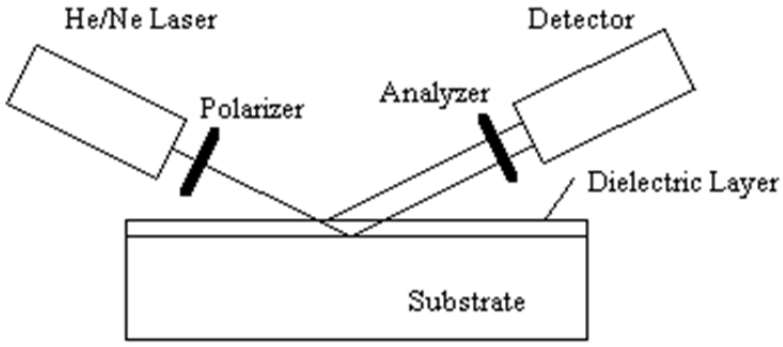

Figure 13: diagram of ellipsometry measurement

One fraction of the photons is directly reflected toward the detector. The other fraction enters a new media with different optical properties to bounce against the reflective substrate and reaches the detector. Since it took more time to reach, the phase of the second photon fraction is different and based on this difference and the parameters entered, the thickness can be calculated. This technique has an Angstrom resolution power, does not require bulky and expensive equipment and is achieve

fairly quickly (a few seconds). It is pretty much universal so long as the substrate is reflecting light and the layer acts as a diaelectric coating. It is also possible to measure 2 layers on the same substrate simultaneously. In another hand, ellipsometry does not give any indication about the chemical composition of the layers. In addition to this, calculations are based on a model chosen by the operator. Inputting the wrong model and parameter would give insignificant results. Following is the model and parameter chosen for our experiments:

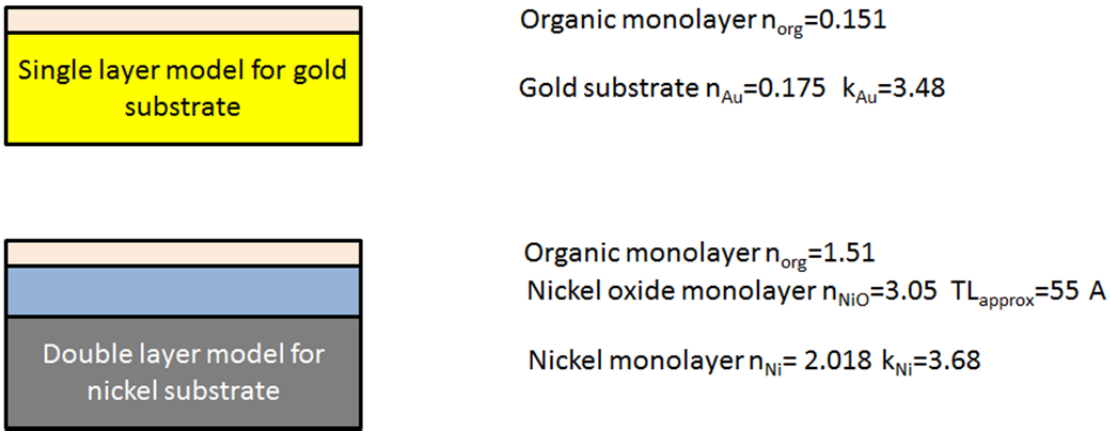

Figure 14: model used for ellipsometry measurement. Incident angle was 70°. n is refractive index; k is the extinction coefficient; TL is the thickness layer.

In addition to ellipsometry, structural analysis must be taken to confirm the SAM formation. To this end, XPS can be used to determine the elemental composition as well as binding information. In XPS analysis, X ray are produced by bombarding a metallic anode with electrons. The X ray then hit the surface of the material to be analyzed and knock out electrons from it. The electrons energy are detected and directly depend on the atom they come from. Electrons from atoms buried in the

material rapidly loose energy and appear as background where the ones coming from the top layers appear as XPS electrons. The analysis is run under high vacuum which means volatile impurities usually do not appear on the substrate. In XPS, one usually runs a survey scan to determine the elements present and then focus on certain range for high resolution and determine binding energy. The energy of the photon is given by hν = KE + BE+ φ_s (KE = kinetic energy; BE = binding energy; hν = x-ray energy; φ_s = spectrometer work function).

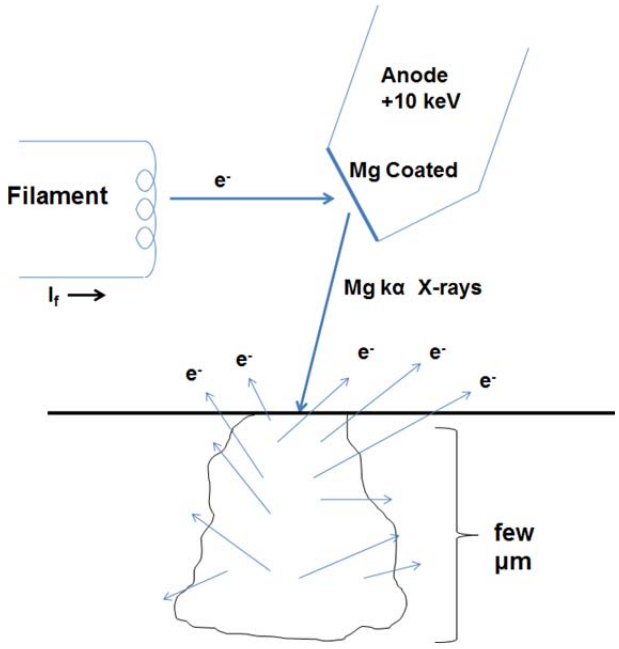

Figure 15: XPS analysis by electrons detection

2.2. Surface chemistry

2.2.1. Thin film preparation

Gold slides were cut and sonicated 15 min in ethanol. Sonication is preferred to piranha solution cleaning because of the compatibility with nanorods. The slides were then coated using chronoamperometry using a platinum ring to close the circuit. Nickel RTU solution was used as provided. The surface of the electrode (exposed gold surface) was 0.9 cm diameter; the current used was 0.2 mA for 1 h. The expected deposited nickel thickness in these conditions is expected to be 258 nm.

2.2.2. Material selective SAM investigation

A 10mM solution of 16-phosphonohexadecanoic acid was prepared by dissolving 34 mg of phosphonic acid in 10.0 mL of water. The solution was sonicated for 1 min. A sonicated gold slide and nickel covered slide were immersed in the solution a heated to 90^{o}C overnight. Similarly, a 10mM solution of 11-mercaptoundecanol was prepared by dissolving 20mg of mercaptol in 10 mL of ethanol. A nickel slide and a gold slide were immersed at room temperature overnight. The slides were then rinsed with clean solvent (water or ethanol), sonicated for a few minutes and dried under N_2. Ellipsometry measurements were taken and XPS analysis of the thiol SAM on gold and phosphonic acid SAM on nickel.

2.2.3. Langmuir rate constant determination

The adsorption rate of thiol on gold and phosphonic acid on nickel oxide was studied by immersing slides in coating agent solution and taking thickness measurement from time to time.

A 10 mM solution of 16-phosphonohexadecanoic acid in water and a 10 mM solution of 11-mercaptoundecanol were prepared as previously described. In addition to this, a 10 mM solution of

mono dodecyl phosphate was prepared by dissolving 27 mg of mono dodecyl phosphate in 10.0 mL of water. A sonicated gold slide was immersed in the thiol solution at room temperature. One nickel coated slide was immersed in each phosphonate solution and heated at 95^{o}C. For each measurement, the slides were removed from the solution, immersed in clean solvent, sonicated for 10 s, rinsed with clean solvent and dried under N_2 for thickness measurement.

2.3. Nanorods synthesis, functionalization and characterization

2.3.1. Nanorods synthesis

Bimetallic nanorods were synthesized by electrodeposition of nickel sulfamate and potassium aurocyanide using an aluminum oxide membrane as a template. Although the membranes used are filtering membranes, which have a diameter of approximately 100 nm, previous experiences show that the internal diameter is closer to 300 nm. The effective surface of the electrode is calculated to be 1.12 cm^2 and with a diameter of 300 nm, yields a maximum of $1.16x10^9$ pores.

One side of the membrane is coated with silver for contact with the electrode. The coated part is placed on a flat piece of platinum and the cell is sealed using a rubber ring. Silver was additionally deposited from a silver succinate solution to further improve the homogeneity in the pore (1.65 mA, 35 min). This layer of silver is referred to as the sacrificial layer. Gold was then deposited using chronoamperometry using 0.33 mA. At this rate, gold is deposited at 18.8 nm/min. The cell was then emptied, thoroughly rinsed with DI water and conditioned with the next solution to be used. Nickel was deposited at a 0.5mA current which correspond to a 9.17 nm/min growth. The growth was slower than the gold one because the molar density is greater.

Once the appropriate size and chain of metal was obtained within the membrane, it was washed with DI water and dried with nitrogen. The sacrificial silver layer was then dissolved in 33% nitric acid by exposing the silver to the solution for 10 s.

The silver-free membrane was then dissolved in 3 M sodium hydroxide for 45 min. The rods were concentrated by centrifugation and re-dispersed in fresh sodium hydroxide solution. This step was repeated twice. Once the membrane was completely dissolved, the nanorods were rinsed with ethanol using the centrifugation/ re-dispersion 3 times, and finally stored in ethanol for analysis with SEM and EDS. The particles are too big to be analyzed by UV (900 nm).

Table 2: Nanorods designation and structure

Nanorods	desired structure
A	Au 400 nm - Ni 400 nm
B	Au 600 nm - Ni 200 nm
C	Au 250 nm- Ni 200 nm- Au 400 nm

2.3.2. Thiolated DNA attachment to gold block

50 µL DNA3 was deprotected like follow.

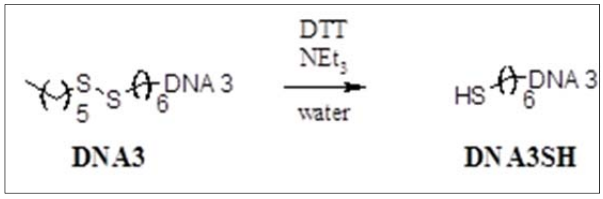

Scheme 2: Deprotection of thiolated DNA

A 0.1 M solution of DTT was prepared by dissolving 15.4 mg of DTT in DI water. 50 µL of a 100 µM solution of thiolated DNA 3 were mixed with 50 µL solution of DTT (1:1000 DNA:DTT molar ratio) and 2µL of triethylamine in a microcentrifuge tube. The mixture was vortexed and allowed to incubate overnight at room temperature. From here, the DNA was isolated and purified using Oligo Clean & Concentrator™ using the following procedure: 100 µL of binding buffer was added to the mixture and homogenized. 400 µL of ethanol was then added to the mixture and the solution was transferred to the spin column. After 30s of centrifugation at 13000 rpm, the flow-through was discarded and 750 µL of wash buffer was added. The column was centrifuged 30 s then 1 min at max speed. The DNA was eluted with 20 µL of DI water to give a final concentration determined by nanodrop UV measurement (135 µM).

The purified and deprotected DNA was diluted to 5 µM solution in a pH 3 buffer (citric acid and disodium phosphate) containing 0.02% of sodium dodecyl sulfate (SDS), 500mM of sodium chloride and 1x tris borate EDTA (TBE). Particles C were dispersed in this solution and mixed for 30 min at

room temperature. The rods were centrifuged at 13000 rpm for 1 min and the liquid was decanted. The excess DNA strands were removed by redispersing the rods in a buffer containing 100 mM of sodium chloride, 0.02% SDS and 1x TBE. After centrifugation, the rods were rinsed in water. Before analysis, the rods were redispersed in ethanol. SEM and EDS were taken in an attempt to confirm the presence of DNA on the gold.

3. Results and Discussion

3.1. Surface chemistry

3.1.1. Thin film characterization

The ellipsometry on gold and nickel was taken to measure the thickness of the layer. The experimental goal here was to show that phosphonates bind to the spontaneously formed nickel oxide layer while showing low affinity to gold and that thiol selectively binds to the gold without attaching to the nickel part.

Phosphonate chains usually tilt at about 28^{o} which means for a 22 Å long molecule (16-phosphonohexadecanoic acid) an increase of roughly 18 Å is expected for a well packed surface. The thiol layer expected thickness is 13 Å (11-mercaptoundecanol).

Table 3: Thickness measurement taken in Angstrom for the different SAM

	Ni surface (upper layer)	Au surface
Before exposure	0.5±0.9 A	4.9±0.2 A
exposure 18h at 90°C in a 10mM solution of 16 phosphonohexadecanoic acid	16.7±0.3 A	6.5±0.2 A
exposure 18h at room temperature in a 10mM solution of 11 mercaptohexanol	0.5±0.9 A	14.8±0.2 A

The results are in line with a well ordered pack SAM in both cases. The low coverage of thiol on nickel and phosphonic acid on gold is consistent to the expected selectivity of the coverage.

The XPS analysis of the thiol on gold confirms the elemental composition and show absence of atomic contaminant. The survey study results with the peaks and their attribution reveal the presence of gold, oxygen, carbon and sulfur. The high resolution XPS in the range of interest gives a better sensitivity and eventually see the overlapping of peaks for the same elements coming from different binding environment.

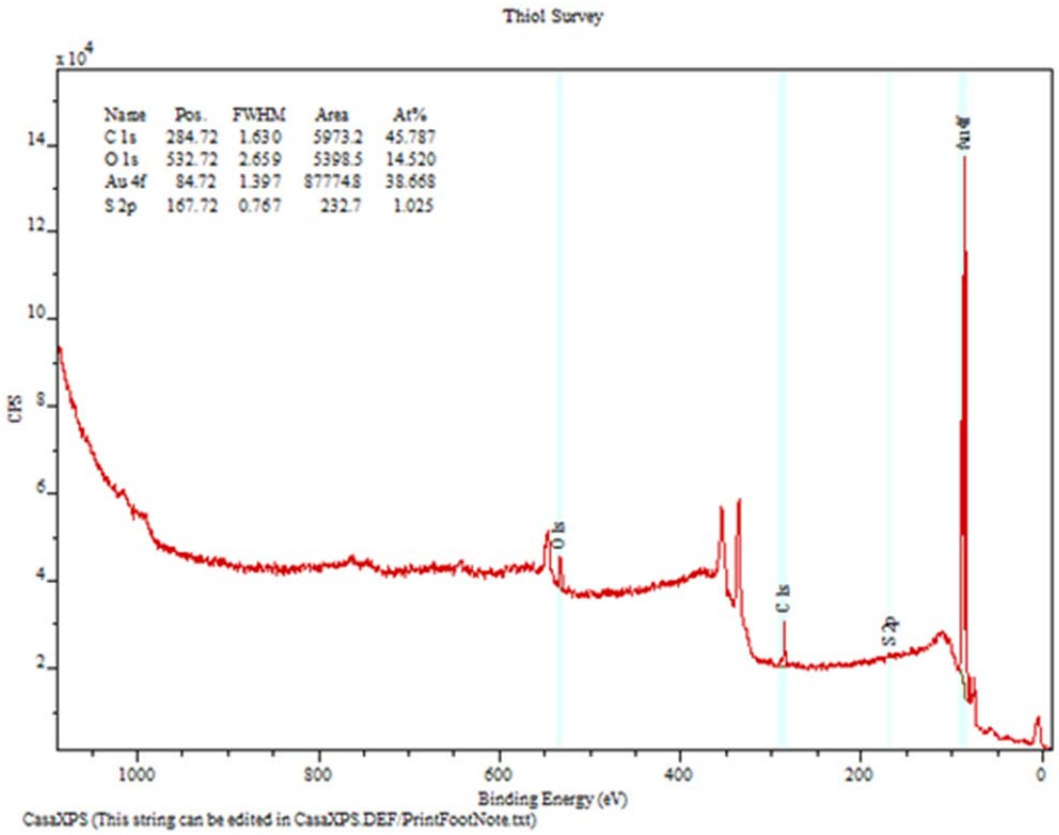

Energy (eV)	1006	774	655	549	531	355	335	285	169	89	85	6
Attribution	C Auger	Au 4s	Au $4p^{1/2}$	Au $4P^{3/2}$	O 1s	Au 4d	Au 4d	C 1s	S 2p	Au 4f	Au 4f	Au

Figure 16: Survey analysis of 11-mercaptoundecanol SAM on gold

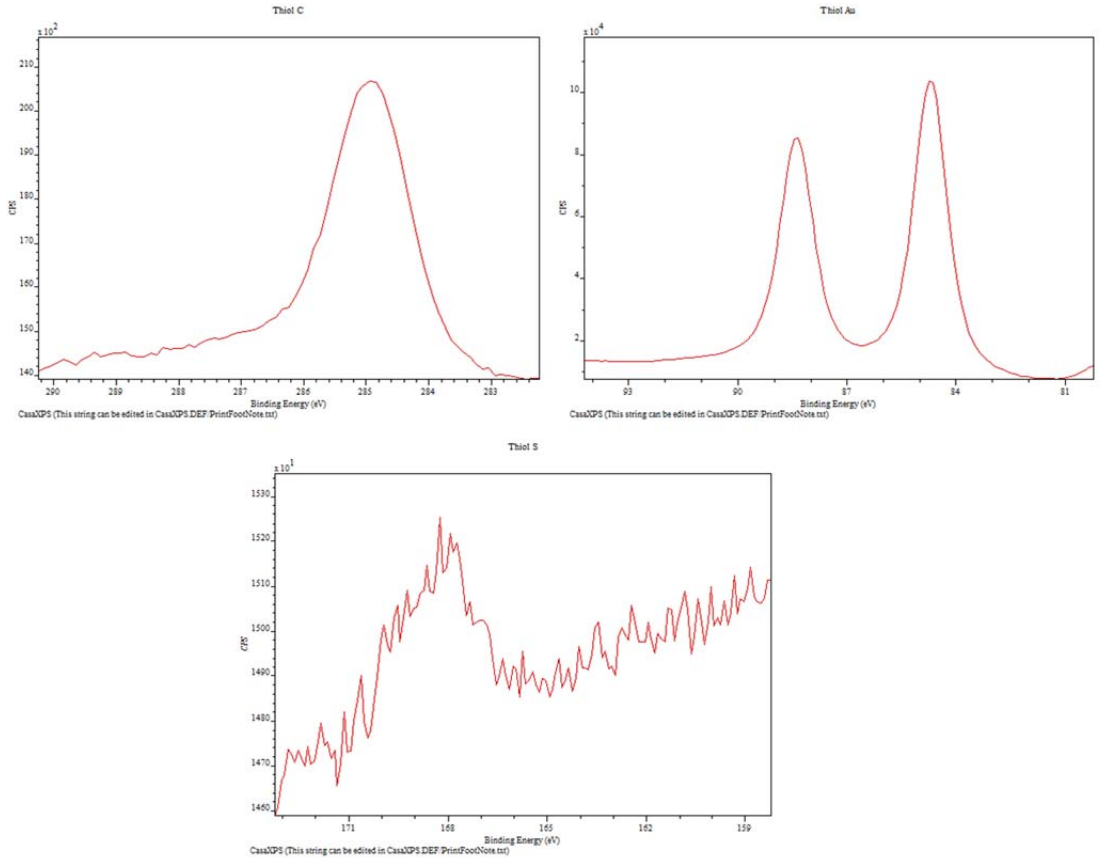

Figure 17: High resolution peaks of different elements in the thiol SAM on gold (C, Au and S)

In this case, the sulfur peak is not intense enough to allow the detection of the binding mode. However, the cleaning process (sonication, multiple washes), the thickness suggesting the packed surface, the high vacuum and finally the literature on the subject allow us to safely assume that the thiol is attach to the gold and that the material on the surface is not caused by nonspecific adsorption.

The data is however less ambiguous in the phosphonic acid on NiO case.

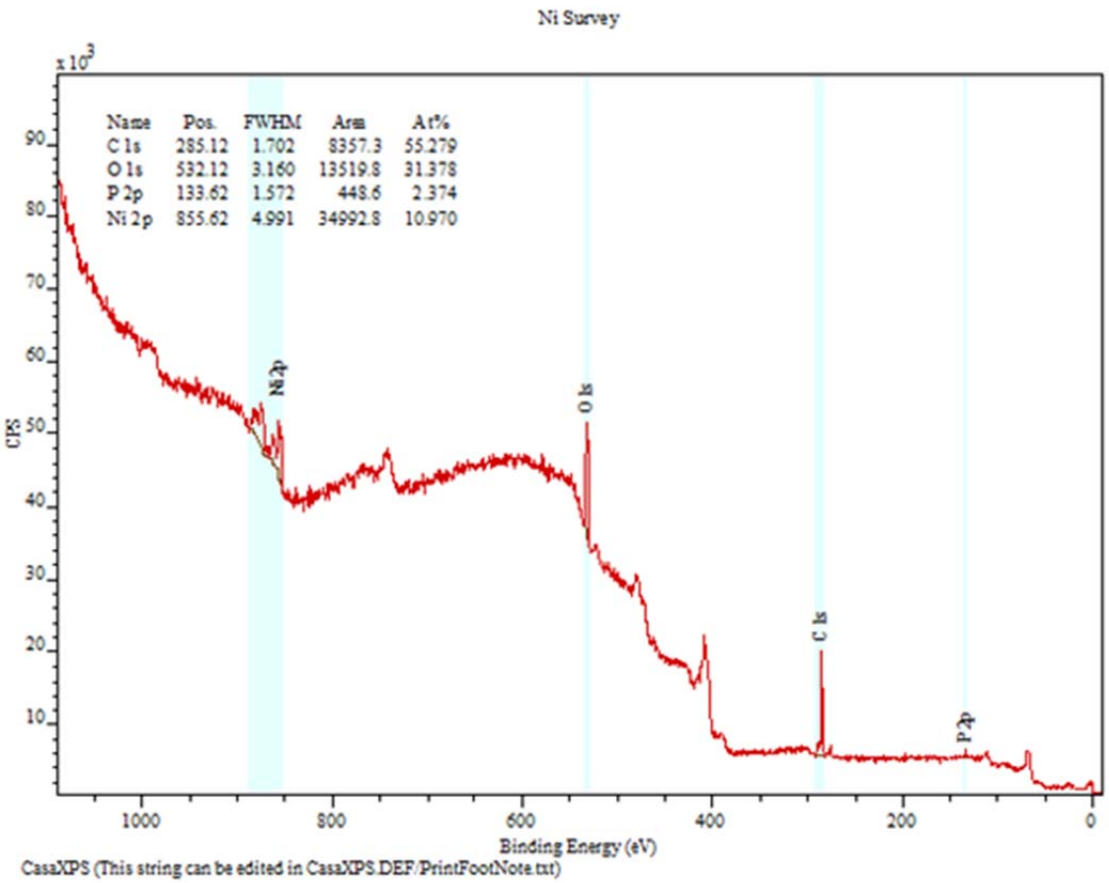

Energy (eV)	1000	872	864	490	418	285	130	120	77
Attribution	C auger	Ni 2p	Ni 2p	Ni auger	Ni auger	C 1s	P 2p	Ni 3s	Ni 3p

Figure 18: Survey analysis of 16-phosphonohexadecanoic acid SAM on nickel

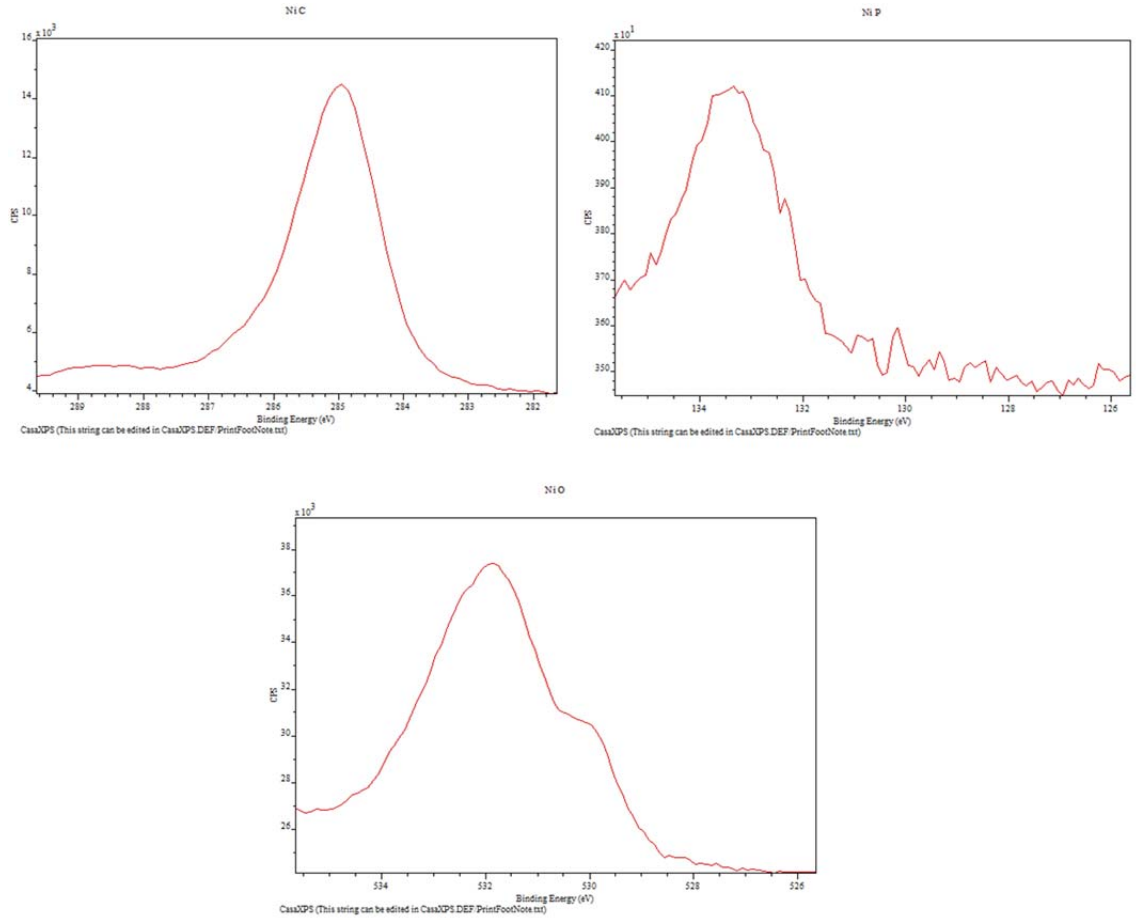

Figure 19: High resolution peaks of different elements in phosphonic acid SAM on nickel (C, P and O)

Again, it should to be noted that there are no impurity peaks coming from atoms other than the one already present on the SAM material. In this case, the oxygen peak profile can be used to extract information about the bonding mode. The shouldering at 530eV is due to the oxygen in the nickel oxide. NiO and Ni-OH are too close to be seen without software analysis but NiO peak tends to be slightly lower than Ni-OH (530.7 vs 531.3 eV).[41] The binding mode of phosphonates on metal oxides has been studied and peak shift between mono, bi and tridentate has been observed (the lower the

binding mode, the higher the energy peak).[42] The 532 eV peak match literature for tridentate binding mode. It is possible to observe the oxygen from the carboxylic acid head group however this one is usually higher in energy around 534 eV and in our case, without software analysis, it is difficult to draw conclusion whether or not the peak is observed. By combining those data with the ellipsometry ones, it is safe to conclude that the phosphonic acid attached to the nickel oxide layer. We now have a method to selectively attach organic molecules to gold and nickel.

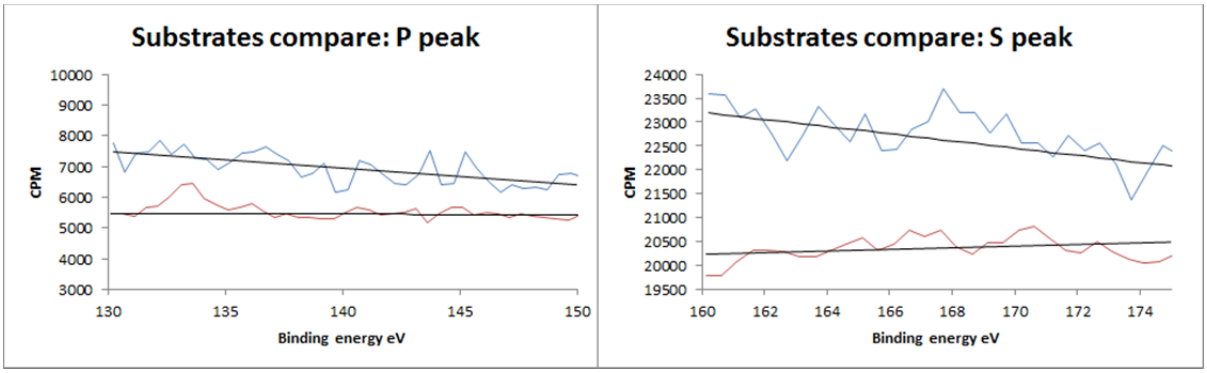

Figure 20: Comparison between the two substrates using the XPS survey. Signal from the gold in blue, signal from the nickel slide in red; background trendline in black. A constant k was added to reduce the separation between the two lines. P peak: 133 eV. S peak: 168 eV

The two surveys spectras have been compared in the phosphorus and thiol range to determine the specificity of the absorption. Although weak, it is clear that no sulfur is detected on the nickel surface and no phosphorus is present on the gold surface.

3.1.2. Langmuir rate law fitting

To optimize the attachment method, the surface coverage speed is measured at several time point of the attachment.

The data are fitted to theoretical value using the following equation: $\theta(t) = 1\text{-}\exp(k_{obs}t)$ where θ is the surface coverage, t is the time and k_{obs} the rate constant. We make the assumptions that we are at high concentration (no diffusion limited kinetic) and that the rate constant of desorption is negligible compare with the adsorption constant.[43]

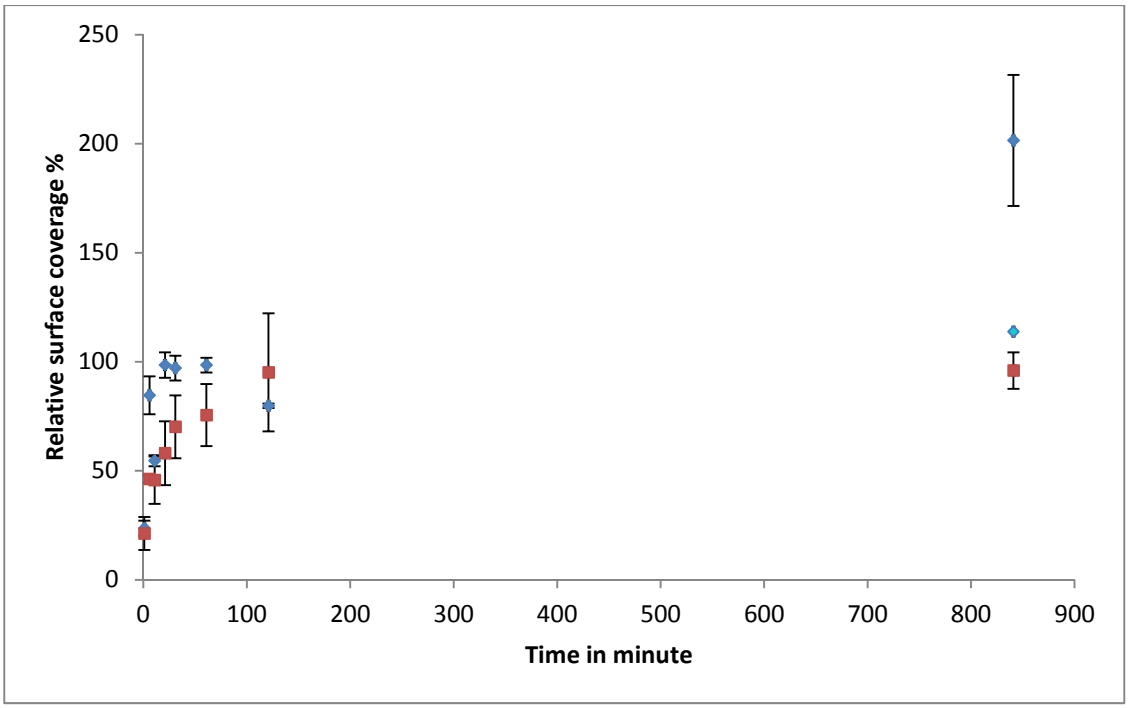

Figure 21: Langmuir rate determination of SAM formation on nickel and gold. In blue, the relative coverage on gold. In red, the relative coverage of nickel surface. The turquoise point is measurement taken on a gold plate that hasn't been removed from the solution for 14 h.

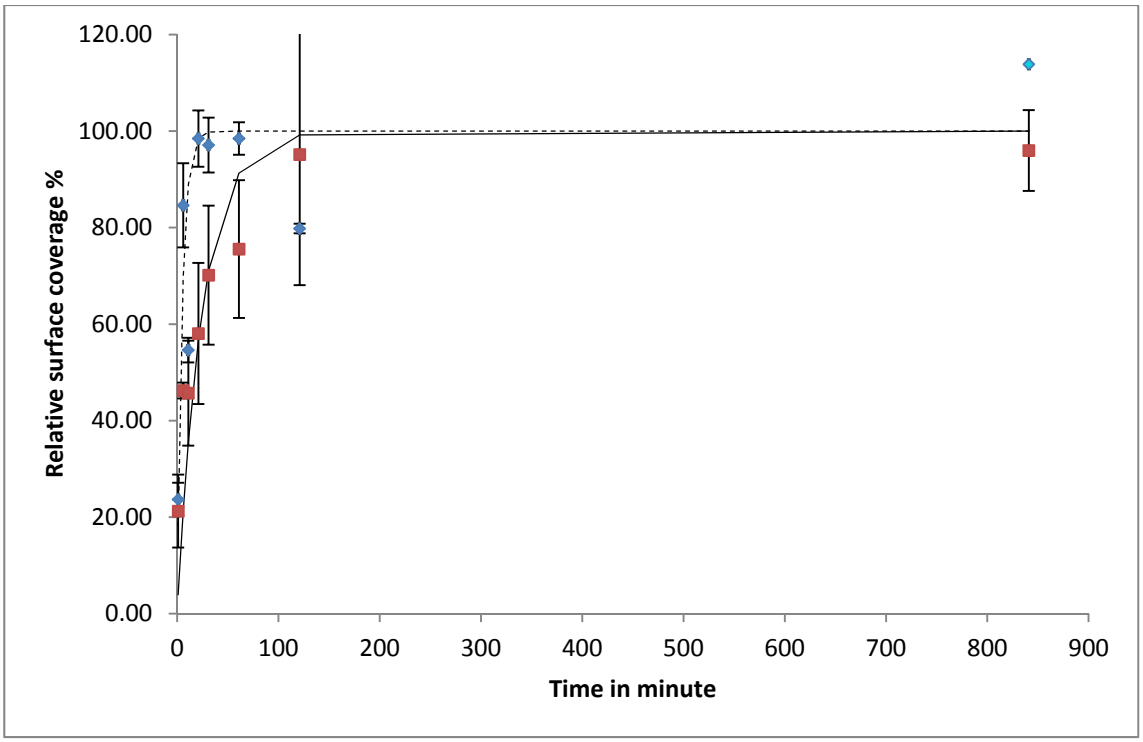

Figure 22: Zoom in the Langmuir rate determination of SAM formation on nickel and gold. In blue, the relative coverage on gold. In red, the relative coverage of nickel surface.

It appears that in the conditions used for the experiment, the thiol covers the surface much faster than the phosphonic acid. Total coverage is reached in 20 min for the thiol where 2 h are needed for the phosphonic acid. It is interesting to observe that the nickel slides exposed to the 11 undecanol phosphate has been completely dissolved overnight. The final recording from the nickel thin film shows unexpected high value. This could be due to an impurity because a similar recording on another plate (which exposure was not interrupted overtime) shows a surface film thickness about 17A. The basic condition combined with the heat might have accelerated the solvation of nickel oxide in the solution. The adsorption constants are found to be 0.2 min^{-1} for the thiol on gold and 0.04 min^{-1} for the phosphonic acid on nickel.

3.2. Nanoparticles analysis

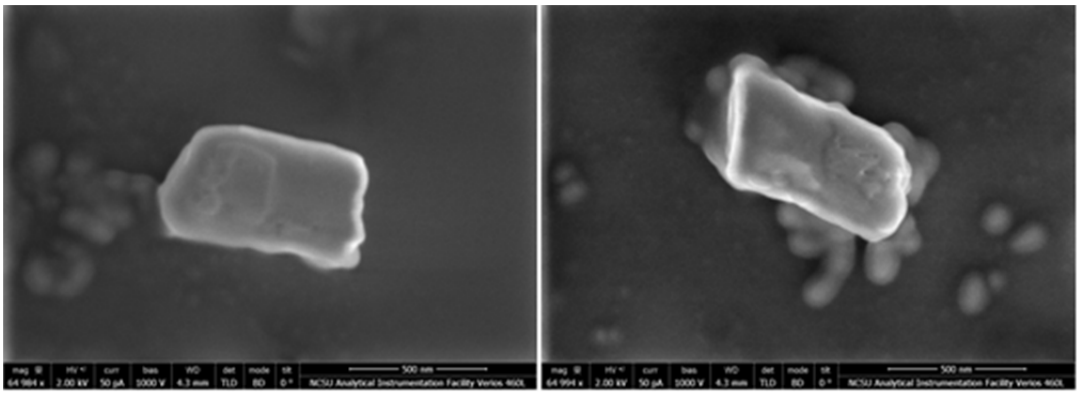

Figure 23: SEM images of particles A

Although it can be observed that the alumina membrane was not completely dissolved, the length of each deposited gold and nickel region is about 380nm which is acceptable compare to expectations. The interface between the two metals can clearly be observed.

In order to determine each metal segment, a 600nm Au – 200 nm Ni was grown and analyzed by SEM and EDS. The small darker section is believed to be nickel while the bright long section should be gold. The difference of color is explained by the fact that the electron density and energy levels are different in metallic gold and nickel. It is also possible that the layer of oxide formed on nickel affects the electron emission. EDS was taken to confirm this hypothesis.

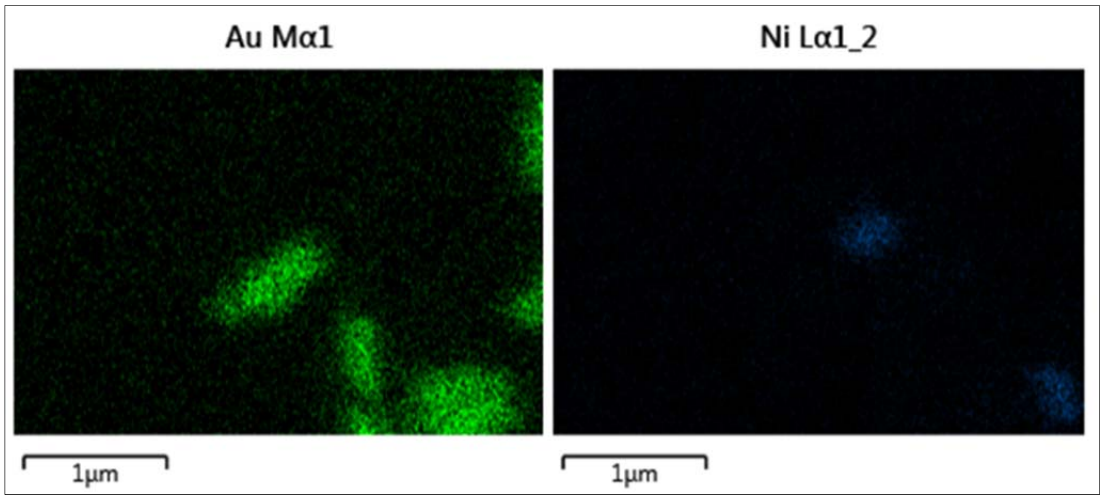

Figure 24: EDS of a nanorod focused on gold (green) and nickel (blue)

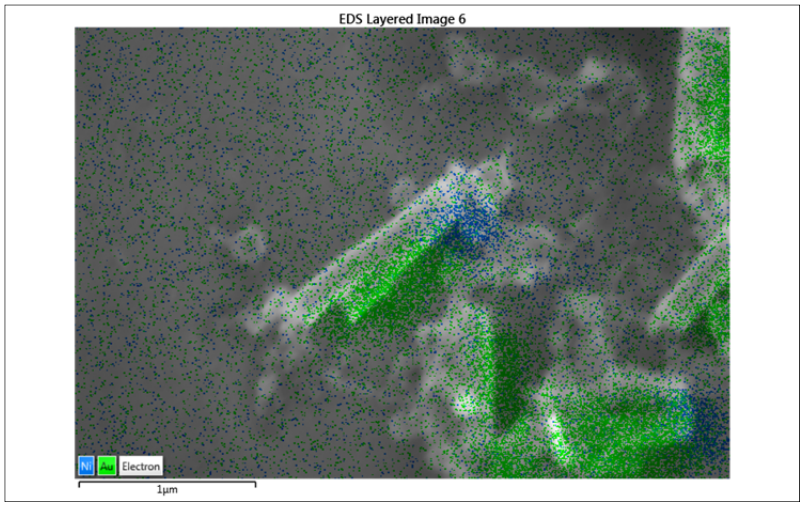

Figure 25: Overlap of the SEM image and the EDS images of the rod

EDS shows the presence of nickel and gold distinctly separated on the particles. This confirms the previously made hypothesis concerning the metal nature. It can be noticed that almost all the rods are

branched. Previous experience has shown that the membranes pores are interconnected to a certain extent, hence the sacrificial layer of electrodeposited silver. It was believed that in this case, not enough silver was deposited. The last rods assembled (particles C) were prepared with a bigger silver sacrificial layer.

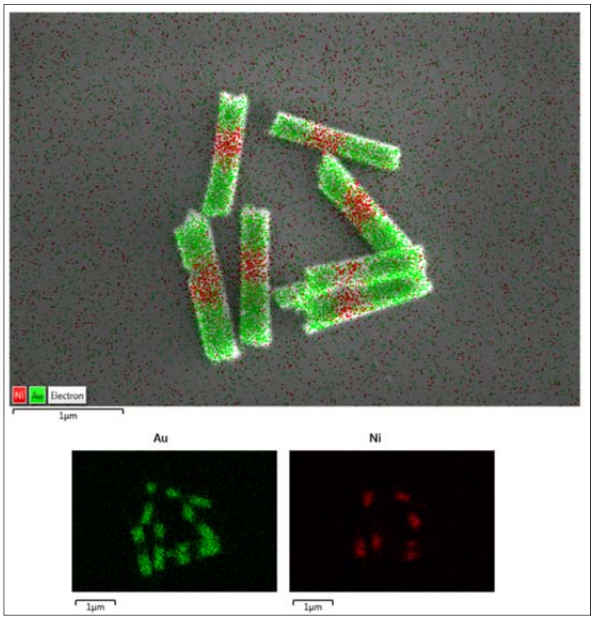

Figure 26: EDS/SEM image of particles C

Since EDS was an elemental analysis, we wanted to track the phosphorus on the surface of the gold block of the nanorods. We found out that phosphorus and gold have X-ray emission overlapping band which means we cannot use phosphorus to track the DNA. Carbon however was not overlapping with gold and although faint, there was definitely a signal on the gold section that was not present on

the nickel section or gold that hasn't been exposed to DNA (although different particles). A coupling reaction was run in parallel to a control experiment in which DNA was absent.

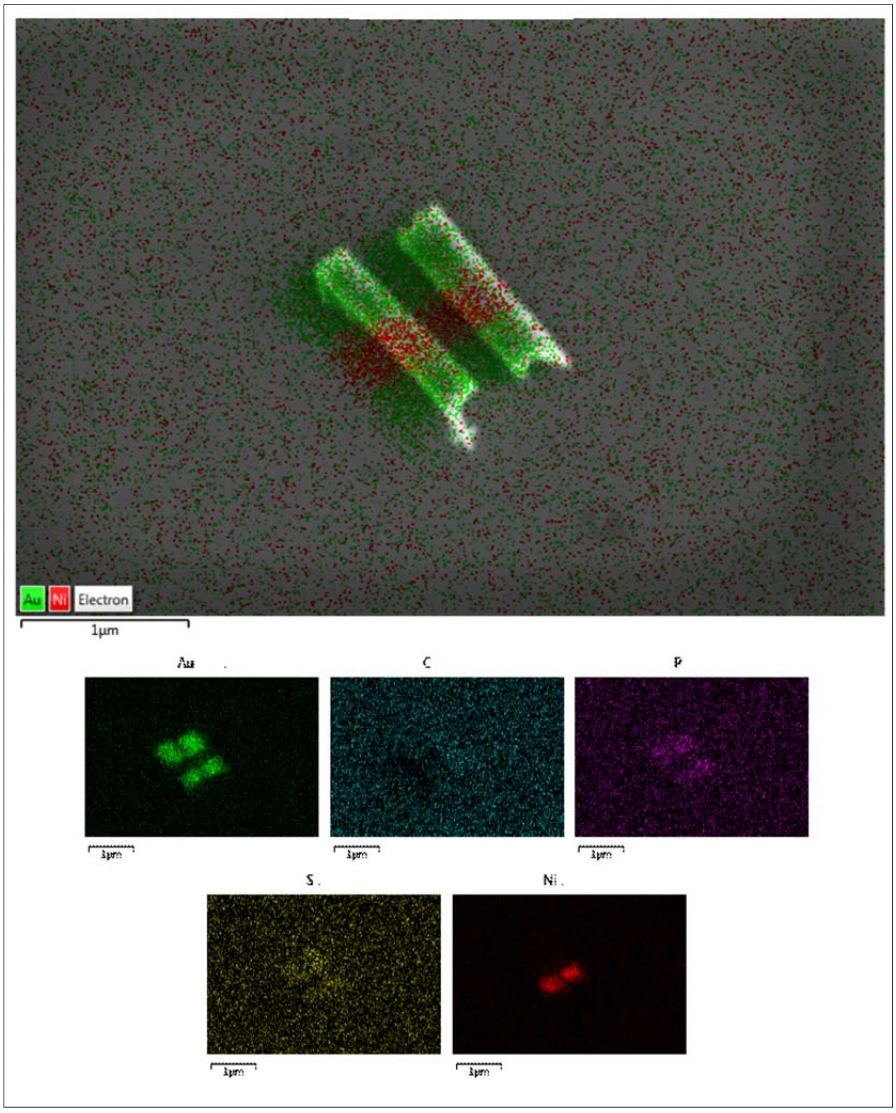

Figure 27: EDS of experiment for DNA coupling

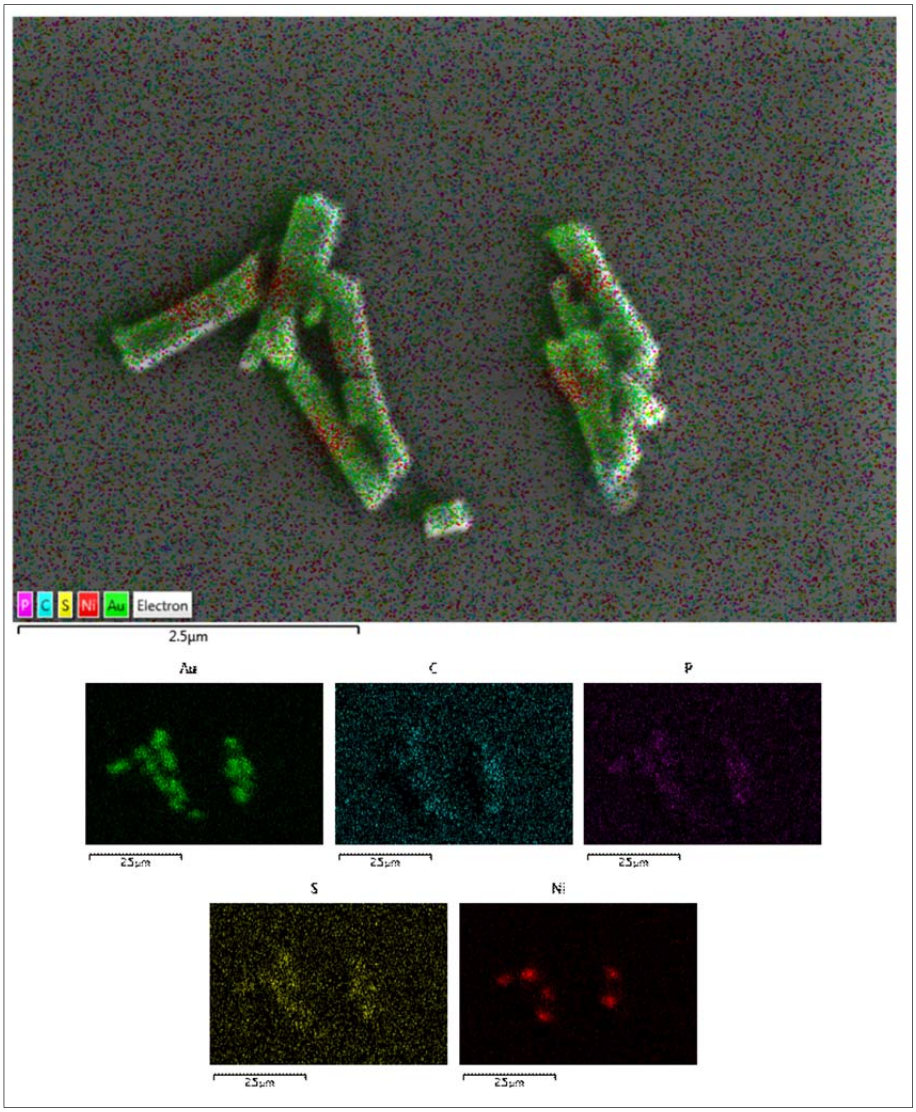

Figure 28: EDS of control for DNA coupling

It appears clearly that both control and experimental have similar elemental signature which means EDS was not a suitable tool for DNA tracking on nanorods surface. However the particles with DNA sample are much more easily redispersed after washing and centrifugation. It could be

explained by the surface charges from the DNA phosphorus backbone which repels each other. This of course is not enough to prove the DNA attachment but much like water affinity on DNA coated surface, it helps in making the assumption that the coupling was successful.

4. Conclusions

The selective functionalization of gold and nickel surfaces has been achieved in conditions suitable with nanorod coating. The method used to characterize the surface can be expended to other metals, alloys, molecules and conditions. Important data concerning the selectivity, the kinetic, the structure of the SAM and the compatibility of the conditions between metals can be obtained. At this point, we have determined that thiols bind selectively to gold and phosphonic acids attach nickel oxide layer through the three oxygen atoms of the anchor group. Langmuir isotherms in the conditions used reveals that thiols cover to gold much faster than phosphonic acids cover the nickel oxide layer.

In addition to this, several nanorods have been synthesized and characterize. It has been found that the membrane internal structure is much wider than expected and branched. Modifying the deposition time though allow to obtain well define straight nanorods. EDS confirm the composition of the nanorods. An attempt of DNA attachment to the gold blocks of nanorods has been carried out but lack of characterization data has not allowed the verification of this DNA attachment on the gold surface. EDS has been found to be unsuitable because its detection level for organic molecules is not low enough. It has to be noted though that the nanorods coated with DNA redispersed much faster in solution. This tends to confirm the hypothesis of DNA attachment because of charge repulsion on the surface although it is not reliable a way to confirm DNA coupling.

This project has tremendous potential to control the orientation and attachment of several nano-objects in bulk solution. With the miniaturization of electronic compounds, such a technique is of interest for future nano-objects assembly.

References

1. Wang, H.; Sun, Z.; Lu, Q.; Zeng, F.; Su, D., One-Pot Synthesis of (Au Nanorod)–(Metal Sulfide) Core–Shell Nanostructures with Enhanced Gas-Sensing Property. *Small 8*, 1167–1172.

2. Murray, W. A.; Barnes, W. L., Plasmonic materials. *Advance Material* **2007,** *19*, 3771–3782.

3. Huang, H.; He, C.; Zeng, Y.; Xia, X.; Yu, X.; Yi, P.; Chen, Z., A novel label-free multi-throughput optical biosensor based on localized surface plasmon resonance. *Biosensors and Bioelectronics* **2009,** *24*.

4. Sepúlveda, B.; Angelomé, P. C.; Lechuga, L. M.; Liz-Marzán, L. M., LSPR-based nanobiosensors. *Nano today* **2009,** *4*, 244-251.

5. Jang, B.; Park, J.-Y.; Tung, C.-H.; Kim, I.-H.; Choi, Y., Gold Nanorod−Photosensitizer Complex for Near-Infrared Fluorescence Imaging and Photodynamic/Photothermal Therapy In Vivo. *ACS Nano* **2011,** *5*, 1086-1094.

6. Zheng, W.; Chase, T. E.; He, L., Multiplexed miRNA detection using cationic polythiophene. *Analytical Methods* **2014,** *6*, 2014.

7. http://www4.ncsu.edu/~lhe2/research.html.

8. Wang, J.; Musameh, M., Carbon nanotube/teflon composite electrochemical sensors and biosensors. *Analytical chemistry* **2003,** *75* (2075-2079).

9. Salem, A. K.; Searson, P. C.; Leong, K. W., Multifunctional nanorods for gene delivery. *Nature Materials* **2007,** *2*, 668-671.

10. (a) Q. Yuan, Z. Z., J. Zhuang, and X. Wang,, Pd-Pt random alloy nanocubes with tunable compositions and their enhanced electrocatalytic activities. *Chemical Communications* **2010,** *46*, 1491–1493; (b) Mu, R.; Fu, Q.; Xu, H.; Zhang, H.; Huang, Y.; Jiang, Z.; Zhang, S.; Tan, D.; Bao, X., Synergetic Effect of Surface and Subsurface Ni Species at Pt-Ni Bimetallic Catalysts for CO Oxidation. *journal of american chemical society* **2011,** *133*, 1978-1986; (c) Yuan, Q.; Zhou, Z.; Zhuang, J.; Wang, X., Seed Displacement, Epitaxial Synthesis of Rh/Pt Bimetallic Ultrathin Nanowires for Highly Selective Oxidizing Ethanol to CO2. *Chemistry of Materials* **2010,** *22*, 2395-2402.

11. Imura, Y.; Tsujimoto, K.; Morita, C.; Kawai, T., Preparation and Catalytic Activity of Pd and Bimetallic Pd−Ni Nanowires. *Langmuir* **2014,** *30*, 5026−5030.

12. Ye, W.; Guo, X.; Xie, F.; Zhu, R.; Zhao, Q.; Yang, J., Kinetics-controlled growth of bimetallic RhAg on Au nanorods and their catalytic properties. *Nanoscale* **2014,** *6*, 4258-4263.

13. Kim, S.-M.; Lee, Y.-J.; Kim, J.-W.; Lee, S.-Y., Facile synthesis of Pt–Pd bimetallic nanoparticles by plasma discharge in liquid and their electrocatalytic activity toward methanol oxidation in alkaline media. *Thin Solid Films* **2014,** *572*, 260-265.

14. http://www.nanoscience.gatech.edu/zlwang/research/nano.html#4.

15. Shankar, K. S.; Raychaudhuri, A. K., Fabrication of nanowires of multicomponent oxides: Review of recent advances. *Materials Science and Engineering: C* **2005,** *25*, 738–751.

16. Hurst, S. J.; Payne, E. K.; Qin, L.; Mirkin, C. A., Multisegmented one-dimensional nanorods prepared by hard-template synthetic methods. *Angewandte Chemie International Edition* **2006,** *45*, 2672–2692.

17. Pena, D. J.; Razavi, B.; Smith, P. A.; Mbindyo, J. K.; Natan, M. J.; Mayer, T. S.; Mallouk, T. E.; Keating, C. D., Electrochemical Synthesis of Multi-Material Nanowires as Building Blocks for Functional Nanostructures. *Material Research Society Symposium* **2001,** *636*.

18. Asaduzzaman, A. M.; Springborg, M., Structural and electronic properties of Au, Pt, and their bimetallic nanowires. *Physical Review B* **2005,** *72*.

19. (a) Keating, C. D.; Natan, M. J., Striped metal nanowires as building blocks and optical tags. *Advance Material* **2003,** *15*, :451–454; (b) Salem, A. K.; Searson, P. C.; Leong, K. W., Multifunctional nanorods for gene delivery. *Nature Materials* **2003,** *2*, 668–671; (c) Liu, F.; Lee, J. Y.; Zhou, W. J., Multisegment PtRu nanorods: Electrocatalysts with adjustable bimetallic pair sites. *Advanced Functional Materials* **2005,** *15*, 1459–1464.

20. Liu, X. H.; Wang, J. Q.; Zhang, J. Y.; Yang, S. R., Sol–gel template synthesis of LiV3O8 nanowires. *Journal of material science* **2007,** *42*, 867-871.

21. http://energyharvesting.pl.

22. Kong, F.-Y.; Xu, B.-Y.; Xu, J.-J.; Chen, H.-Y., Simultaneous electrochemical immunoassay using CdS/DNA and PbS/DNA nanochains as labels. *Biosensors and Bioelectronics* **2013,** *39* 177–182.

23. Gazit, E., Use of biomolecular templates for the fabrication of metal nanowires. *FEBS Journal* **2007,** *274*, 317–322.

24. Love, J. C.; Estroff, L. A.; Kriebel, J. K.; Nuzzo, R. G.; Whitesides, G. M., Self-Assembled Monolayers of Thiolates on Metals as a Form of Nanotechnology. *Chemical Reviews* **2005,** (105), 1103-1169.

25. (a) D.Evans, S.; Ulman, A., Surface potential studies of alkyl-thiol monolayers adsorbed on gold. *Chemical Physics Letters* **1990,** *170* (5,6), 462; (b) Widrig, C. A.; C. Chung; Porter, M. D., The electrochemical desorption of n-alkanethiol monolayers from polycrystalline Au and Ag electrodes. *Journal of Electroanalytical Chemistry* **1991**, 335-359.

26. (a) Malinsky, M. D.; Kelly, K. L.; Schatz, G. C.; Duyne, R. P. V., Chain Length Dependence and Sensing Capabilities of the Localized Surface Plasmon Resonance of Silver Nanoparticles Chemically Modified with Alkanethiol Self-Assembled Monolayers. *Journal of american chemical society* **2001,** *123*, 1471-1482; (b) Shon, Y.-S.; Dawson, G. B.; Porter, M.; Murray, R. W., Monolayer-Protected Bimetal Cluster Synthesis by Core Metal Galvanic Exchange Reaction. *Langmuir* **2002,** *18*, 3880–3885.

27. Häkkinen, H., The gold–sulfur interface at the nanoscale. *Nature chemistry* **2012,** *4*, 443-455.

28. Herne, T. M.; Tarlov, M. J., Characterization of DNA Probes Immobilized on Gold Surfaces. *Journal of american chemical society* **1997,** *119*, 8916–8920.

29. Rajalingam, S.; Devillers, S.; Dehalle, J.; Mekhalif, Z., A two step process to form organothiol self-assembled monolayers on nickel surfaces. *Thin Solid Films* **2012,** *522*, 247–253.

30. Iida, M.; Ohtsuka, T., Ellipsometry of passive oxide films on nickel in acidic sulfate solution. *Corrosion Science* **2007,** *49*, 1408.

31. Birenbaum, N. S.; Lai, B. T.; Chen, C. S.; Reich, D. H.; Meyer, G. J., Selective Noncovalent Adsorption of Protein to Bifunctional Metallic Nanowire Surfaces. *Langmuir* **2003,** *19*, 9580-9582.

32. Quiñones, R.; Raman, A.; Gawalt, E. S., Functionalization of nickel oxide using alkylphosphonic acid self-assembled monolayers. *Thin Solid Films 516* **2008,** *516*, 8774–8781.

33. Cabrita, J. F.; Viana, A. S.; Montforts, F.-P.; Abrantes, L. M., Mixed self-assembled monolayers of Co-porphyrin and n-alkane phosphonates on gold. *Surface Science* **2011,** *605*, 1412–1419.

34. Liu, H.; Pierre-Pierre, N.; Huo, Q., Dynamic light scattering for gold nanorod size characterization and study of nanorod – protein interactions. *Gold bulletin* **2012,** *45*, 187–195.

35. Ahmad, R.; Boubekeur-Lecaque, L.; Nguyen, M.; Lau-Truong, S.; Lamouri, A.; Decorse, P.; Galtayries, A.; Pinson, J.; Felidj, N.; Mangeney, C., Tailoring the Surface Chemistry of Gold

Nanorods through Au−C/Ag−C Covalent Bonds Using Aryl Diazonium Salts. *Journal of Physical Chemistry C* **2014,** *118*, 19098−19105.

36. https://www.phi.com/surface-analysis-techniques/tof-sims.html.

37. Shi, D.; Song, C.; Jiang, Q.; Wang, Z.-G.; Ding, B., A facile and efficient method to modify gold nanorods with thiolated DNA at a low pH value. *Chemical Communications* **2013,** *49*, 2533--2535.

38. Bauer, L. A.; Reich, D. H.; Meyer, G. J., Selective Functionalization of Two-Component Magnetic Nanowires. *Langmuir* **2003,** *19*, 7043-7048.

39. Nerambourg, N.; H.V., M.; Charlot, M.; Blanchard-Desce, M., Quenching of Molecular Fluorescence on the Surface of Monolayer-Protected Gold Nanoparticles Investigated Using Place Exchange Equilibria. *Langmuir* **2007,** *23*, 5563–5570.

40. (a) Quiñones, R.; Raman, A.; Gawalt, E. S., Functionalization of nickel oxide using alkylphosphonic acid self-assembled monolayers. *Thin Solid Films* **2008,** *516*, 8774–8781; (b) Noel, S.; Houze, F.; Boyer, L.; Mekhalif, Z.; Delhalle, J.; Caudano, R., Self-Assembled Monolayers of Alkanethiols on Nickel Surfaces for Low Level Electrical Contact Applications. *IEEE Transactions on components and packaging technology* **1999,** *22*, 79-84.

41. http://srdata.nist.gov/xps/EngElmSrchQuery.aspx?EType=PE&CSOpt=Retri_ex_dat&Elm=O.

42. (a) Timpel, M.; Nardi, M. V.; Krause, S.; Ligorio, G.; Christodoulou, C.; Pasquali, L.; Giglia, A.; Frisch, J.; Wegner, B.; Moras, P.; Koch, N., Surface Modification of ZnO(0001)−Zn with Phosphonate-Based Self-Assembled Monolayers: Binding Modes, Orientation, and Work Function. *Chemistry of Materials* **2014,** *26*, 5042−5050; (b) Brancha, B.; Dubeyb, M.; Andersonc, A. S.; Artyushkovaa, K.; Baldwind, J. K.; Petseva, D.; Dattelbaumd, A. M., Investigating phosphonate monolayer stability on ALD oxide surfaces. *Thin Solid Films* **2014,** *288*, 98– 108.

43. Hu, K.; Bard, A. J., In Situ Monitoring of Kinetics of Charged Thiol Adsorption on Gold Using an Atomic Force Microscope. *Langmuir* **1988,** *14*, 4790-4794.